## FULL PAPERS

Virtual domains! Using molecular dynamics (MD) simulations, the importance of structured water molecules in bromodomains, an important class of emerging drug targets, was investigated. The results show that structured water molecules in the acetyl-lysine binding site can be replaced by cosolvent molecules. This result has important implications for the design of selective drugs against bromodomain targets.
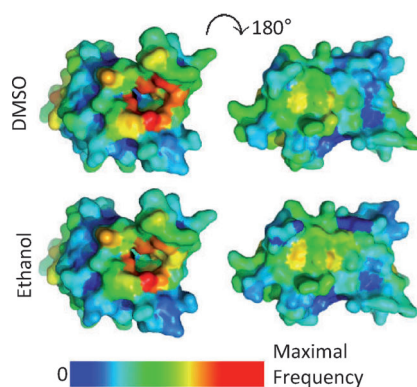
D. Huang,* E. Rossini, S. Steiner,
A. Caflisch*

■■ – ■■

Structured Water Molecules in the Binding Site of Bromodomains Can Be Displaced by Cosolvent

Structured Water Molecules in the Binding Site of Bromodomains Can Be Displaced by Cosolvent

Danzhi Huang,* Emanuele Rossini, Sandra Steiner, and Amedeo Caflisch*[a]

Bromodomains are α-helical bundles of approximately 110 residues that recognize acetylated lysine side chains mainly on histone tails. Bromodomains are known to play an important role in cancer and inflammation, and as such, significant efforts are being made to identify small-molecule inhibitors of these epigenetic reader proteins. Here, explicit solvent molecular dynamics (MD) simulations of two bromodomains (BAZ2B and CREBBP) are used to analyze the water molecules that seem to be conserved at the bottom of the acetyl-lysine binding site in most crystal structures of bromodomains. The MD runs suggest that the occupancy of the structured water molecules is influenced by conformational transitions of the loop that connects helices Z and A. Additional simulations in the presence of 50 molecules of cosolvent (i.e., 440 mM of dimethylsulfoxide, methanol, or ethanol) indicate that some of the structured water molecules can be displaced transiently. The residence time in the acetyl-lysine binding site is calculated to be about 1 ns, 2–5 ns, and 10–30 ns for methanol, ethanol, and dimethylsulfoxide, respectively, while the affinity of the three cosolvents for BAZ2B and CREBBP is in the range of 50–500 mM. The results described have implications for ligand design, suggesting that only structured water molecules that do not exchange with cosolvent should be maintained in crystal structures used for docking campaigns, and that hydroxy substituents should be incorporated in the ligand so as to map the structured water molecules replaced by (m)ethanol.

Introduction

Bromodomains bind acetylated lysine side chains mainly in histones and are thus involved in the regulation of transcription.[1,2] As of today, 46 human proteins have been reported to include one or more of the 61 different bromodomains, with up to six bromodomains per protein.[3] As some bromodomains play an important role in cancer and inflammation,[4–6] there is an intense search for small-molecule inhibitors able to interfere in the process of reading acetylated lysine.[7] The first three-dimensional structure of a human bromodomain was solved by nuclear magnetic resonance spectroscopy.[8] Since then, the crystal and/or solution structures of more than 40 human bromodomains have been published.[9,10] All available structures show a conserved four-helix bundle topology (Figure 1a) in which the ZA-loop and BC-loop connect the first two α helices (Z and A) and last two α helices (B and C), respectively.[10,11] The acetyl-lysine binding site is very similar in all structures of bromodomains.[10] It is substantially hydrophobic but contains at its bottom several well-ordered water molecules (Figure 1b), which are present in most crystal structures of bromodomains.[7,10] In striking contrast to the abundance of available three-dimensional structures, to date, there have only been a few computational studies reported in the literature on bromodomains.[12–14] In particular, it seems that the dynamic properties of human apo bromodomains have not been investigated yet by atomistic simulations except for a very recent simulation study of 20 bromodomains.[15] On the other hand, several approaches to map (co)solvent to protein surfaces have been developed using protocols based on energy minimization[16–20] and more recently molecular dynamics (MD).[21–28]

Here, explicit solvent MD simulations are performed to analyze the occupancy of the conserved water molecules in the acetyl-lysine binding site and their potential displacement by dimethylsulfoxide (DMSO) or alcohol cosolvents ethanol and methanol. DMSO and ethanol differ mainly in the capability to act as a hydrogen-bond donor—only ethanol is able to do so. Methanol was selected for study because it differs in a single methylene group from ethanol, which provides information on size effects and hydrophobic-effect-dominated binding. Two bromodomains belonging to two different families are used in the simulations: the bromodomain adjacent to zinc finger domain 2B (BAZ2B) and the binding protein of the cAMP response element binding protein (CREBBP). There are several examples of explicit solvent MD simulations of small molecules binding to proteins.[22,23,29–33] On the other hand, the present work is the first simulation analysis of cosolvent binding to bromodomains. The simulation results reveal that the conformational changes of the ZA-loop are likely to have an influence on water occupancy. Moreover, the results suggest that some of the water molecules that are conserved in the available crystal structures of bromodomains can be transiently replaced by cosolvent molecules. This information is very useful

[a] D. Huang, E. Rossini, S. Steiner, Prof. A. Caflisch
Department of Biochemistry, University of Zürich
Winterthurerstrasse 190, 8057 Zürich (Switzerland)
E-mail: dhuang@bioc.uzh.ch
caflisch@bioc.uzh.ch
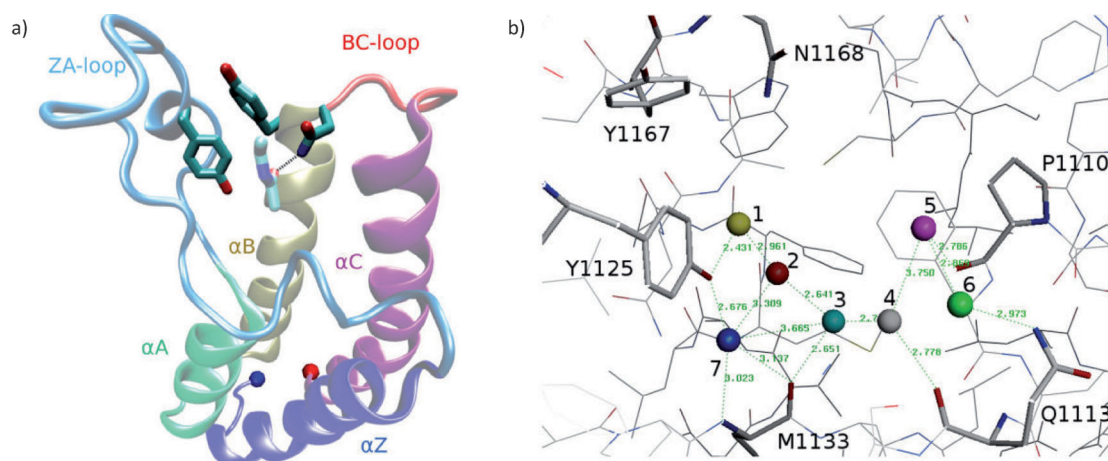
Figure 1. Bromodomain structure and structured water molecules in the bottom of the acetyl-lysine binding site. a) Ribbon illustration of the crystal structure of the complex between CREBBP and acetyl-lysine (PDB code: 3P1C[10]). Each of the four α-helices and two binding site loops is displayed with a different color. The side chains of the conserved residues Tyr 1125 of the ZA-loop, and Tyr 1167–Asn 1168 of the BC-loop are emphasized (sticks) together with the acetyl-lysine ligand (sticks, light colors). The N and C termini are shown with a blue and red sphere, respectively. The structure of BAZ2B (not shown) is very similar to that of CREBBP. The conserved residues in BAZ2B are Tyr 1901 in the ZA-loop, and Phe 1943–Asn 1944 in the BC-loop. b) Positions of structured water molecules. Water molecules 1–6 are the same as described in Ref. [7].

for hit identification by high-throughput docking and hit optimization based on docking models.[34–45] Our simulation results suggest to keep only the structured water molecules that do not exchange with cosolvent in high-throughput docking campaigns. Moreover, the position of structured water molecules that are replaced by (m)ethanol can be used to design hydroxy substituents of initial hits, which can improve the affinity by up to two orders of magnitude.[46–48]

Results
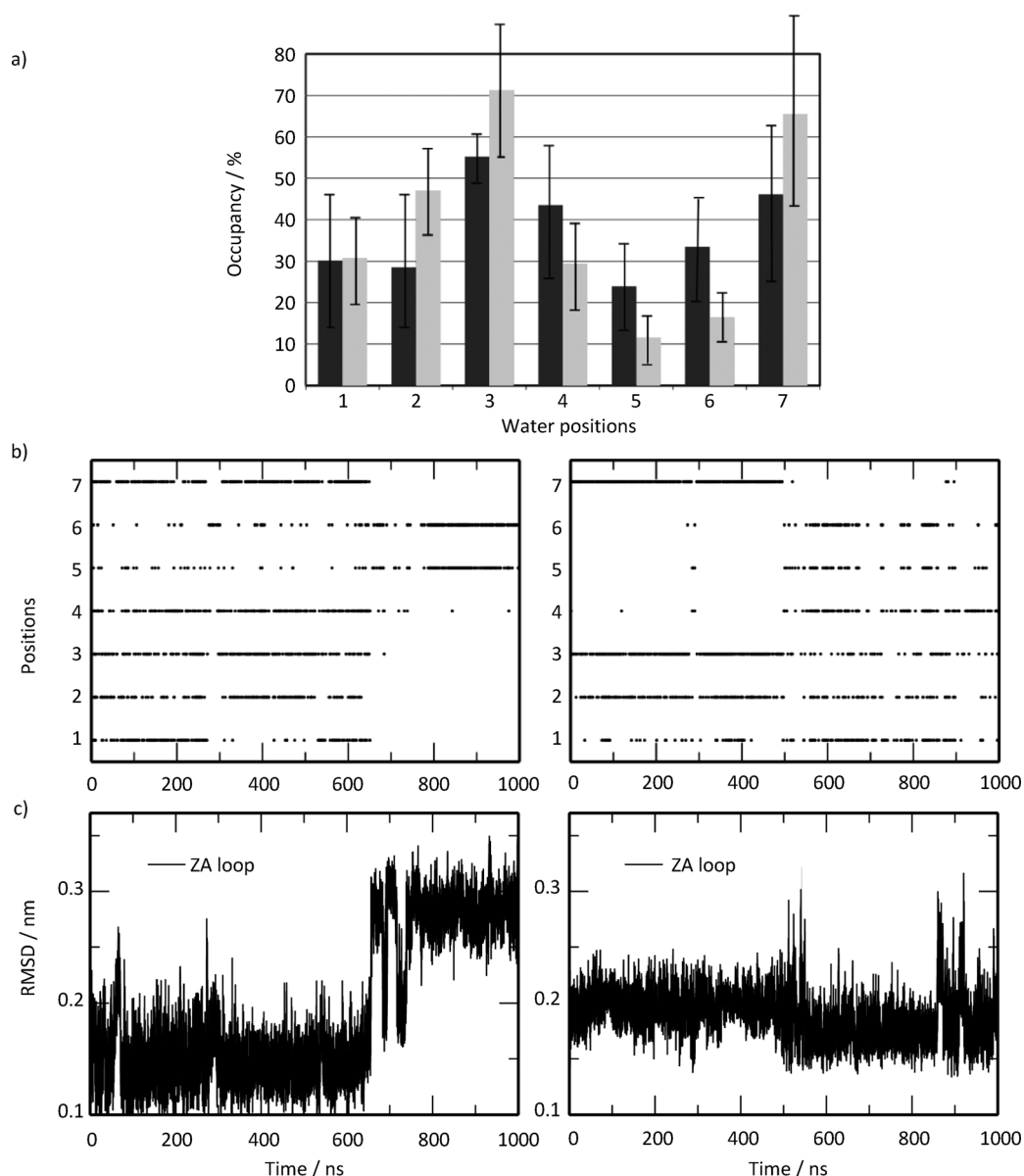
Simulations without cosolvent

For each of the structured water molecules, the occupancy was calculated using a threshold value for the distances between the water oxygen atom and three (mainly) backbone atoms in the acetyl-lysine binding site (Table S1 in the Supporting Information). The positions of water molecules 3 and 7 have the highest occupancy in the simulations of both bromodomains, while the position of water molecule 5 has the lowest occupancy (Figure 2). These simulation results are consistent with the degree of burial observed in the crystal structures,[7] which is maximal for water molecules 3 and 7. The time evolution of the water occupancy and root mean square deviation (RMSD) of the ZA-loop from its position in the crystal structure show a similar pattern (Figure 2), which indicates that the presence of the conserved water molecules is influenced by the motion of the ZA-loop. The structured water molecules connected by hydrogen bonds (i.e., water molecules 1–3) show similar temporal patterns of occupancy. In other words, these three water molecules are either all present or all absent along the simulation. The same behavior is observed for water molecules 5 and 6, which are also connected by a hydrogen bond. On the other hand, water molecule 4 can have temporal

evolution of the occupancy similar as water molecules 1–3 or 5–6.

Simulations with cosolvent

These simulations were started from random positions of 50 cosolvent molecules in the bulk water and without any cosolvent molecule in the acetyl-lysine binding site. The maps of cosolvent occupancy (Figure 3) indicate that DMSO, ethanol, and methanol bind preferentially to the acetyl-lysine binding site. From these maps, it also emerges that methanol can bind to most of the bromodomain surface. Methanol is less specific than ethanol and DMSO because it is the smallest of these three cosolvents, and furthermore, in contrast to DMSO, it can also act as a hydrogen-bond donor.

The time series of the distance of the DMSO molecule closest to the acetyl-lysine binding site of CREBBP demonstrates that the MD sampling is adequate as multiple binding and unbinding events are observed and by different DMSO molecules in the 0.5 μs time scale of the MD runs (Figure 4). Cluster analysis of the MD trajectories show that the most populated binding modes of DMSO and (m)ethanol are consistent with the crystal structure of DMSO bound to CREBBP (PDB code: 3P1E[10]) and 1,2-ethanediol bound to the second bromodomain of TAF1 (PDB code: 3UV4[10]), respectively (Figure 4). (Note that there are no crystal structures of CREBBP and BAZ2B with alcohol cosolvent in the acetyl-lysine binding pocket and no crystal structure of DMSO–BAZ2B.) In their most populated binding mode, DMSO, ethanol, and methanol accept a hydrogen bond from the side chain of the same asparagine residue that is involved in binding the natural ligand acetyl-lysine (Figure 4).

These are not the final page numbers! ↗↗

Figure 2. Water occupancy in the simulations without cosolvent. a) Percentage of water occupancy at each of the seven positions shown in Figure 1b. Each bar shows the average and standard deviation calculated over four independent simulations without cosolvent for a total of 4 μs for each of the two proteins (■ BAZ2B; ▨ CREBBP). b) Time series of occupancy of positions of structured water molecules along one of the four 1 μs MD runs for BAZ2B (left) and CREBBP (right). c) Time series of RMSD from the crystal structure of the carbon atoms in the ZA loop upon structural overlap of the carbon atoms of residues in nonflexible parts of the bromodomain. These two panels show results for the same MD runs shown in panel b.

Discussion

As mentioned above, the analysis of the occupancy of the structured water molecules in the presence of cosolvent is useful for docking and hit optimization. The seven structured water molecules are present in the most populated binding mode of the cosolvent while they can be displaced for more buried binding modes. The time series of water or cosolvent occupancy (Figure 5; see also Figure S1 in the Supporting Information) show that the cosolvent displaces mainly the structured water molecules at positions 1 and 5. In addition, there is transient displacement of water molecules 2–4 and 6 by methanol and ethanol. In contrast, the deeply buried water molecule 7 is displaced much less frequently by cosolvent. For example, with BAZ2B, the displacement of individual structured water molecules by ethanol is observed in 10%, 0.3%, 0.5%, 0.1%, 4%, 0.3%, and 0% of the MD sampling for positions 1–7, respectively (for other values of cosolvent occupancy, see Table S2 in the Supporting Information).

The sampling of multiple binding and unbinding events allows one to extract the kinetics directly from the MD simulations (Table 1). The binding and unbinding times are calculated from the fitting of the respective cumulative distribution (Figure S2 in the Supporting Information) as in a previous MD study of the (un)binding of cosolvent molecules from the FK506 binding protein.[32,33] The binding times are similar

These are not the final page numbers! ↗↗
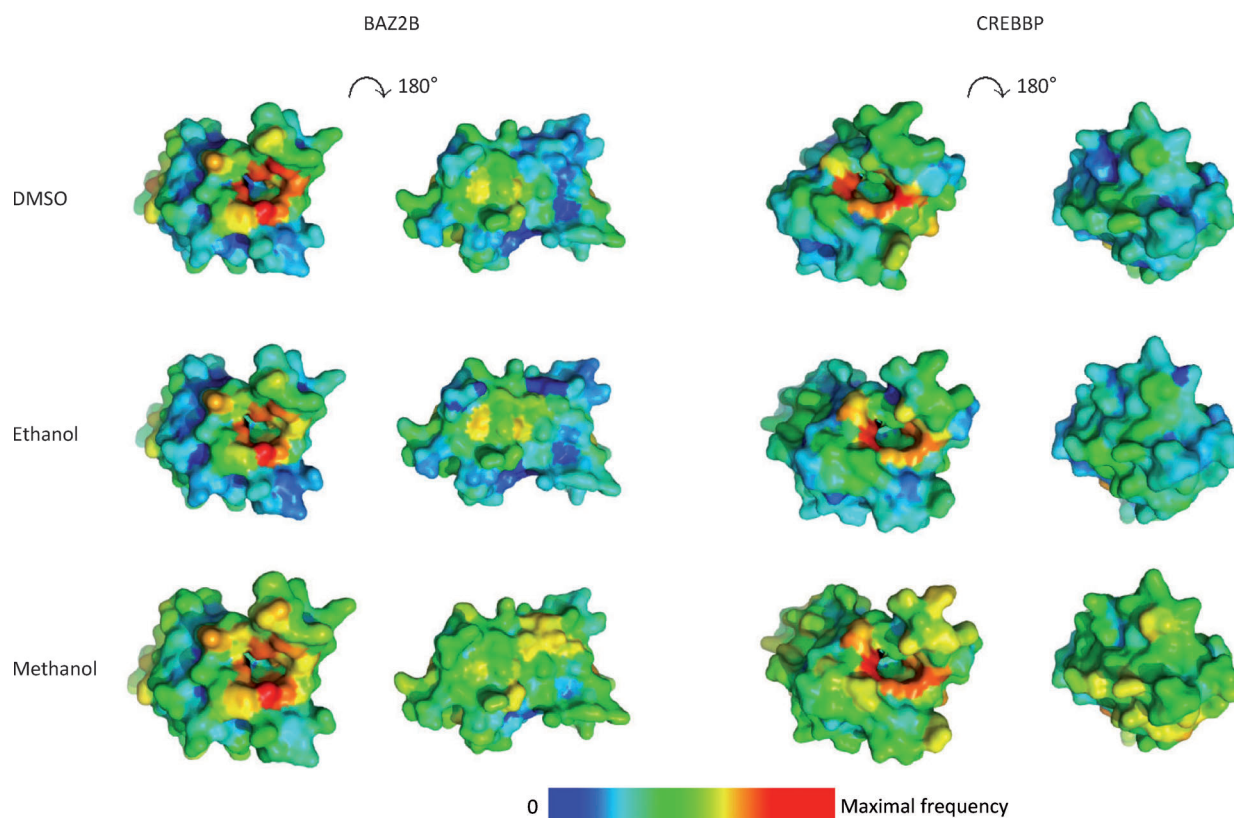
Figure 3. Maps of cosolvent/bromodomain contact frequencies. The surface of the protein is colored according to the percentage of MD snapshots in which the center of mass of any of the 50 molecules of cosolvent is within 0.7 nm of any nonhydrogen atom of the protein. The structures in the first and third columns are oriented such that the acetyl-lysine binding pocket is perpendicular to the plane of the image. The structures in the second and fourth columns are obtained by 180° rotation around a horizontal axis in the plane of the image. These maps show that, for all three cosolvents and both bromodomains, the acetyl-lysine binding pocket is the main binding site.

(factor of five between the slowest and fastest) for the three cosolvents and two bromodomains, which is a consequence of diffusion-limited binding as the three cosolvents used in this study have similar size and polarity. Methanol, the smallest of the three cosolvents investigated here, has the lowest occupancy of the acetyl-lysine binding site for both bromodomains, which is due to its short residence times (about 1 ns). DMSO and ethanol have higher occupancy than methanol because of longer residence time (2.4–26 ns) and similar binding time. The slower unbinding of DMSO and ethanol with respect to methanol might be a consequence of their slightly larger size and/or hydrophobicity. Each of the three cosolvents has similar unbinding times for the two bromodomains. The only exception is the three times longer unbinding time of DMSO from CREBBP compared with BAZ2B. It is interesting to note that this simulation result is consistent with the higher affinity of DMSO for CREBBP than for BAZ2B (Table 1), as measured by a peptide-displacement assay[4,49] with AlphaScreen technology.[50] The experimental results indicate how strongly DMSO competes with an acetylated histone peptide that is a known ligand of the corresponding bromodomain. Note that the competition experiments do not measure directly the cosolvent dissociation constant and therefore a perfect agreement between experimental measurements and dissociation constants derived from the simulations is not expected.

Conclusions

The simulations of bromodomains in pure water show that the occupancy of the conserved water molecules depends on the orientation of the ZA-loop. In the simulations with cosolvent, most of the structured water molecules at the bottom of the acetyl-lysine binding pocket can be transiently displaced by ethanol or methanol. The heterogeneous occupancy of the structured water molecules revealed by the MD simulations is helpful for ligand design, for example, in deciding which of the structured water molecules to take into account for high-throughput docking campaigns. Furthermore, the water molecules displaced by (m)ethanol can be used directly in ligand design, where the inclusion of hydroxy substituents in the ligand so as to map the positions of these displaced structured water molecules could give rise to an increase in binding affinity.

Experimental Section

Simulation protocols: The coordinates of CREBBP and BAZ2B were downloaded from the protein database (PDB codes: 3DWY[10] and 3G0L[2], respectively).[51] To reproduce neutral pH conditions, the side chains of aspartates and glutamates were negatively charged, those of lysine and arginine residues were positively charged, and

These are not the final page numbers! ↗↗
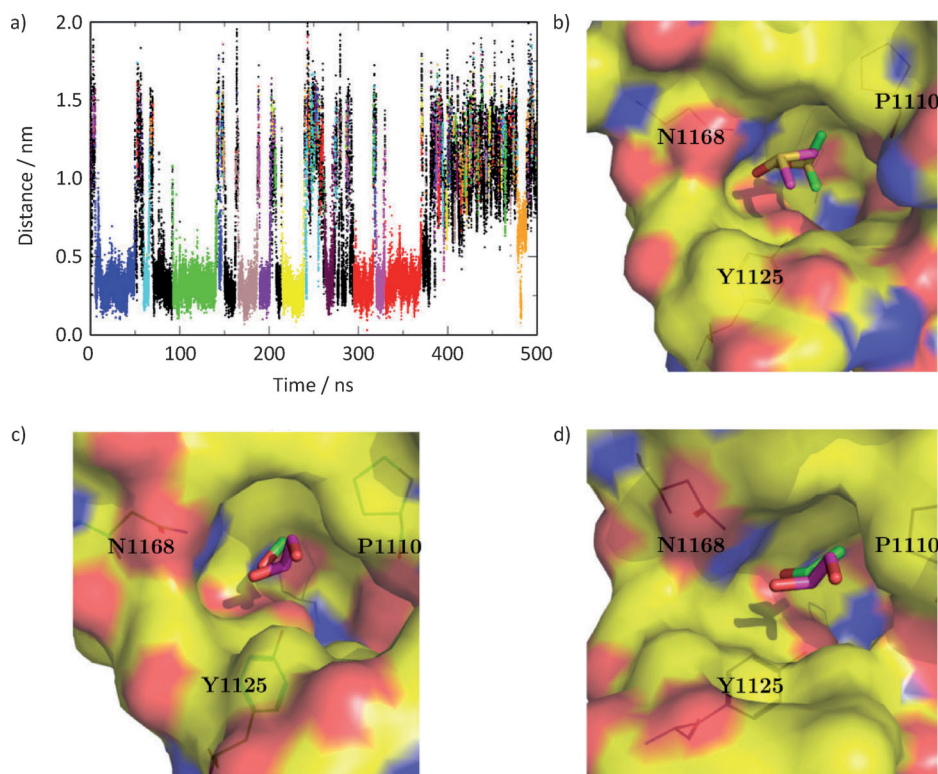
Figure 4. Reversible binding and major binding modes. a) Time series of distance between the center of the acetyl-lysine binding site in CREBBP and the closest DMSO molecule. Different DMSO molecules are "labeled" by different colors. b) The most populated binding mode of DMSO from the MD simulations of CREBBP. DMSO is shown by sticks colored by atomic element (O: red; S: yellow; C: green (pose obtained by MD) or magenta (binding mode in crystal structure PDB code: 3P1E[10]). The surface of CREBBP is colored by atomic element (C: yellow; N: blue; O: red). The same is shown for c) methanol and d) ethanol. The pose obtained by MD for methanol and ethanol is similar to the binding mode of 1,2-ethanediol (C atoms in magenta) in the second bromodomain of TAF1 (PDB code: 3UV4[10]).
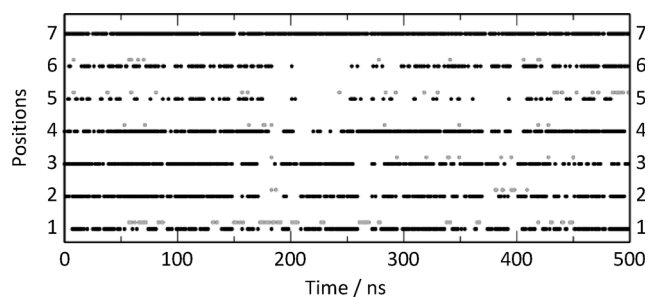
Figure 5. Water displacement by cosolvent: Time series of occupancy of ethanol (grey dots) or water (black dots) at each of the seven positions of structured water molecules along one of the two simulations of BAZ2B carried out in the presence of 50 molecules of ethanol molecules.

the histidine side chains were neutral. For each bromodomain, the crystal water molecules close to the binding site and with low B factor values were kept while the remaining water molecules were deleted. Subsequently, the structure was solvated in a water box, the size of which was chosen to have a minimal distance of 1.1 nm between the boundary and any atom of the protein. Fifty molecules of methanol, ethanol, or dimethylsulfoxide (DMSO) corresponding to a concentration of 440 mм were placed randomly in the bulk water. Solvation water molecules within 0.24 nm of any heavy atom of the protein or the cosolvent were removed. Sodium

and chloride ions, the parameters for which are from the CHARMM PARAM22 force field,[52] were added randomly by replacing noncrystallographic water molecules to compensate for the total charge of each bromodomain and to approximate an ionic strength of about 150 mм. The MD simulations were carried out with Gromacs 4.5.5[53] using the CHARMM PARAM22 force field[52] and the TIP3P model of water.[54] Parameters for the three cosolvents were determined according to the CHARMM general force field.[55]

Periodic boundary conditions were applied and electrostatic interactions were evaluated using the particle-mesh Ewald summation method.[56] The van der Waals interactions were truncated at a cutoff of 1.0 nm. The MD simulations were performed at constant temperature (310 K) using the velocity rescaling thermostat and constant pressure (1 atm).[57] The LINCS algorithm was used to fix the covalent bonds involving hydrogen atoms, and a time step of 2 fs was used in all runs. Before each MD simulation, the whole system was relaxed by energy minimization until the maximal force on individual atoms was smaller than 100 kJ mol^{-1} nm^{-1}. After the minimization, initial atomic velocities, corresponding to the Boltzmann distribution at a temperature of 310 K, were randomly assigned and a constrained MD run was performed for 1 ns. During the constrained simulations, heavy atoms of the protein were fixed to their initial positions with a force constant of 1000 kJ mol^{-1} nm^{-1}. The constraints were released, and the system was equilibrated for 10 ns before data collection for analysis. For each of the two bromodomains (CREBBP and BAZ2B), four independent 1 μs MD runs without cosolvent were carried out. In addition, two independent MD runs of 0.5 μs each were performed for each of the six cosolvent/bromodomain systems. Details of the simulation protocol are given in the Supporting Information.

Analysis: The analysis of the MD trajectories was carried out with CHARMM[58] and the MD analysis tool WORDOM.[59] Occupancy of each of the seven positions of the structured water molecules was determined using the triplets of binding site atoms listed in Table S1 in the Supporting Information.

Clustering according to pairwise RMSD of the cosolvent atoms was carried out using the leader algorithm as implemented in WORDOM. First, the structural overlap was determined using the bromodomain carbon atoms excluding those in the flexible regions, i.e., the ZA and BC loops and the five terminal residues. Upon overlap of the bromodomain structures, the RMSD was evaluated for the nonhydrogen atoms of the cosolvent molecule closest to the acetyl-lysine binding site. A threshold value of 0.2 nm for

These are not the final page numbers! ↗↗

Table 1. Thermodynamics and kinetics of cosolvent binding.							
				Simulation results			Experimental data
Protein	Cosolvent	τ_{on} [ns]	τ_{off} [ns]	k_{off}/k_{on}[a] [mM]	Occupancy[b] [%]	K_D[c] [mM]	Affinity[d] [mM]
BAZ2B	methanol	1.1	0.9	543	54	375	–
	ethanol	0.7	2.4	124	82	97	–
	DMSO	2.6	8.9	128	67	218	347
CREBBP	methanol	0.5	1.3	176	55	360	–
	ethanol	1.0	4.5	94	86	71	–
	DMSO	2.1	26	36	75	147	18

[a] Dissociation constant evaluated as the quotient of k_{off} and k_{on} which are derived from fitting of the cumulative distributions of unbinding times and binding times, respectively (Figure S2 in the Supporting Information). The characteristic time of the slow phase of the double-exponential fitting is used to calculate the binding rate $k_{on} = 1/(\tau_{on}[\text{cosolvent}])$ and unbinding rate $k_{off} = 1/\tau_{off}$. The concentration of the cosolvent in the simulation box is 440 mM. The distance between the binding site center and the mass center of the cosolvent is used to monitor binding. The binding site center of CREBBP is defined by the geometric center of the carbon α atoms of residues Pro 1110, Pro 1114, Tyr 1125, and Asn 1168. The binding site center of BAZ2B is defined by the geometric center of the carbon α atoms of residues Pro 1888, Pro 1892, Tyr 1901 and Asn 1944. The threshold distances used for the calculations of binding and unbinding times are 0.4 nm and 0.8 nm, respectively. Results with different cutoff combinations are listed in Table S3 in the Supporting Information. Using binding cutoffs in the range 0.3–0.5 nm and unbinding cutoffs in the range 0.7–0.9 nm results in differences in K_D smaller than a factor of three. [b] The occupancy of the active site was determined using the same threshold for the distance between the binding site center and the mass center of the cosolvent as for the unbinding kinetics (0.8 nm). [c] Dissociation constant (K_D) calculated from occupancy of acetyl-lysine binding site using $K_D = [\text{cosolvent}]$ [unbound protein]/[bound protein] = [cosolvent] (100−occupancy)/occupancy. The robustness of the occupancy upon changes in the threshold is shown in Figure S3 in the Supporting Information. Using threshold values ranging from 0.5 to 0.9 nm results in differences in K_D smaller than a factor of two. [d] Experimental value of binding affinity measured by AlphaScreen peptide displacement assay.[4,49]

the RMSD from the cluster representative was used for assigning a snapshot to a cluster.

Acknowledgements

[1] L. Zeng, M.-M. Zhou, FEBS Lett. 2002, 513, 124–128.
[2] P. Filippakopoulos, S. Knapp, FEBS Lett. 2012, 586, 2692–2704.
[3] C. H. Arrowsmith, C. Bountra, P. V. Fish, K. Lee, M. Schapira, Nat. Rev. Drug Discovery 2012, 11, 384–400.
[4] P. Filippakopoulos, J. Qi, S. Picaud, Y. Shen, W. B. Smith, O. Fedorov, E. M. Morse, T. Keates, T. T. Hickman, I. Felletar, M. Philpott, S. Munro, M. R. McKeown, Y. Wang, A. L. Christie, N. West, M. J. Cameron, B. Schwartz, T. D. Heightman, N. L. Thangue, C. A. French, O. Wiest, A. L. Kung, S. Knapp, J. E. Bradner, Nature 2010, 468, 1067.
[5] J. Zuber, J. Shi, E. Wang, A. R. Rappaport, H. Herrmann, E. A. Sison, D. Magoon, J. Qi, K. Blatt, M. Wunderlich, M. J. Taylor, C. Johns, A. Chicas, J. C. Mulloy, S. C. Kogan, P. Brown, P. Valent, J. E. Bradner, S. W. Lowe, C. R. Vakoc, Nature 2011, 478, 524–528.
[6] M. A. Dawson, T. Kouzarides, B. J. Huntly, N. Engl. J. Med. 2012, 367, 647–657.
[7] D. S. Hewings, T. P. C. Rooney, L. E. Jennings, D. A. Hay, C. J. Schofield, P. E. Brennan, S. Knapp, S. J. Conway, J. Med. Chem. 2012, 55, 9393–9413.
[8] C. Dhalluin, J. E. Carlson, L. Zeng, C. He, A. K. Aggarwal, M.-M. Zhou, Nature 1999, 399, 491–496.
[9] S. Mujtaba, L. Zeng, M. Zhou, Oncogene 2007, 26, 5521–5527.
[10] P. Filippakopoulos, S. Picaud, M. Mangos, T. Keates, J.-P. Lambert, D. Barsyte-Lovejoy, I. Felletar, R. Volkmer, S. Müller, T. Pawson, A.-C. Gingras, C. H. Arrowsmith, S. Knapp, Cell 2012, 149, 214–231.
[11] L. R. Vidler, N. Brown, S. Knapp, S. Hoelder, J. Med. Chem. 2012, 55, 7346–7359.
[12] S. Pantano, A. Marcello, A. Ferrari, D. Gaudiosi, A. Sabò, V. Pellegrini, F. Beltram, M. Giacca, P. Carloni, Proteins 2006, 62, 1062–1073.
[13] F. Pizzitutti, A. Giansanti, P. Ballario, P. Ornaghi, P. Torreri, G. Ciccotti, P. Filetici, J. Mol. Recognit. 2006, 19, 1–9.
[14] K. D. Eichenbaum, Y. Rodriguez, M. Mezei, R. Osman, Proteins Struct. Funct. Bioinf. 2010, 78, 447–456.
[15] S. Steiner, A. Magno, D. Huang, A. Caflisch, FEBS Lett. 2013, in press; DOI: 10.1016/j.febslet.2013.05.032
[16] A. Miranker, M. Karplus, Proteins Struct. Funct. Genet. 1991, 11, 29–34.
[17] A. Caflisch, A. Miranker, M. Karplus, J. Med. Chem. 1993, 36, 2142–2167.
[18] D. Joseph-McCarthy, J. Hogle, M. Karplus, Proteins Struct. Funct. Bioinf. 1997, 29, 32–58.
[19] C. Stultz, M. Karplus, Proteins Struct. Funct. Genet. 1999, 37, 512–529.
[20] M. Scarsi, N. Majeux, A. Caflisch, Proteins Struct. Funct. Bioinf. 1999, 37, 565–575.
[21] R. Baron, J. A. McCammon, Biochemistry 2007, 46, 10629–10642.
[22] J. Seco, F. J. Luque, X. Barril, J. Med. Chem. 2009, 52, 2363–2371.
[23] O. Guvench, A. D. MacKerell, Jr., PLoS Comput. Biol. 2009, 5, e1000435.
[24] K. W. Lexa, H. A. Carlson, Q. Rev. Biophys. 2012, 45, 301–343.
[25] R. Baron, J. A. McCammon, Annu. Rev. Phys. Chem. 2013, 64, 151–175.
[26] P. Setny, R. Baron, P. M. Kekenes-Huskey, J. A. McCammon, J. Dzubiella, Proc. Natl. Acad. Sci. USA 2013, 110, 1197–1202.
[27] K. W. Lexa, H. A. Carlson, J. Chem. Inf. Model. 2013, 53, 391–402.
[28] K. W. Lexa, H. A. Carlson, J. Am. Chem. Soc. 2011, 133, 200–202.
[29] D. Ekonomiuk, X.-C. Su, C. Bodenreider, S. P. Lim, G. Otting, D. Huang, A. Caflisch, J. Med. Chem. 2009, 52, 4860–4868.
[30] N. Basse, J. L. Kaar, G. Settanni, A. C. Joerger, T. J. Rutherford, A. R. Fersht, Chem. Biol. 2010, 17, 46–56.
[31] I. Buch, T. Giorgino, G. D. Fabritiis, Proc. Natl. Acad. Sci. USA 2011, 108, 10184–10189.
[32] D. Z. Huang, A. Caflisch, ChemMedChem 2011, 6, 1578–1580.
[33] D. Z. Huang, A. Caflisch, PLoS Comput. Biol. 2011, 7, e1002002.
[34] C. Poornima, P. Dean, J. Comput.-Aided Mol. Des. 1995, 9, 521–531.
[35] W. E. Minke, D. J. Diller, W. G. Hol, C. L. Verlinde, J. Med. Chem. 1999, 42, 1778–1788.
[36] R. L. Mancera, J. Comput.-Aided Mol. Des. 2002, 16, 479–499.
[37] C. de Graaf, P. Pospisil, W. Pos, G. Folkers, N. P. Vermeulen, J. Med. Chem. 2005, 48, 2308–2318.
[38] M. L. Verdonk, G. Chessari, J. C. Cole, M. J. Hartshorn, C. W. Murray, J. W. M. Nissink, R. D. Taylor, R. Taylor, J. Med. Chem. 2005, 48, 6504–6515.

[39] C. Barillari, J. Taylor, R. Viner, J. W. Essex, *J. Am. Chem. Soc.* **2007**, *129*, 2577–2587.

[40] R. Abel, T. Young, R. Farid, B. J. Berne, R. A. Friesner, *J. Am. Chem. Soc.* **2008**, *130*, 2817–2831.

[41] J. Michel, J. Tirado-Rives, W. L. Jorgensen, *J. Am. Chem. Soc.* **2009**, *131*, 15403–15411.

[42] D. D. Robinson, W. Sherman, R. Farid, *ChemMedChem* **2010**, *5*, 618–627.

[43] T. Beuming, Y. Che, R. Abel, B. Kim, V. Shanmugasundaram, W. Sherman, *Proteins Struct. Funct. Bioinf.* **2012**, *80*, 871–883.

[44] N. G. M. Davies, H. Browne, B. Davis, M. J. Drysdale, N. Foloppe, S. Geoffrey, B. Gibbons, T. Hart, R. Hubbard, M. R. Jensen, H. Mansell, A. Massey, N. Matassova, J. D. Moore, J. Murray, R. Pratt, S. Ray, A. Robertson, S. D. Roughley, J. Schoepfer, K. Scriven, H. Simmonite, S. Stokes, A. Surgenor, P. Webb, M. Wood, L. Wright, P. Brough, *Bioorg. Med. Chem.* **2012**, *20*, 6770–6789.

[45] S. Riniker, L. J. Barandun, F. Diederich, O. Krämer, A. Steffen, W. F. van Gunsteren, *J. Comput.-Aided Mol. Des.* **2012**, *26*, 1293–1309.

[46] K. Lafleur, D. Huang, T. Zhou, A. Caflisch, C. Nevado, *J. Med. Chem.* **2009**, *52*, 6433–6446.

[47] H. Zhao, J. Dong, K. Lafleur, C. Nevado, A. Caflisch, *ACS Med. Chem. Lett.* **2012**, *3*, 834–838.

[48] K. Lafleur, J. Dong, D. Huang, A. Caflisch, C. Nevado, *J. Med. Chem.* **2013**, *56*, 84–96.

[49] Conference notes on the lecture of P. Brennan, RSC Advances in Synthesis and Medicinal Chemistry, Welwyn Garden City, UK, May 1st, **2012**.

[50] R. M. Eglen, T. Reisine, P. Roby, N. Rouleau, C. Illy, R. Bossé, M. Bielefeld, *Curr. Chem. Genomics* **2008**, *1*, 2–10.

[51] F. C. Bernstein, T. F. Koetzle, G. J. Williams, E. F. Mayer, Jr., M. D. Brice, J. R. Rodgers, O. Kennard, T. Shimanouchi, M. Tasumi, *Arch. Biochem. Biophys.* **1978**, *185*, 584–591.

[52] A. D. MacKerell, Jr., D. Bashford, M. Bellott, R. L. Dunbrack, Jr., J. D. Evanseck, M. J. Field, S. Fischer, J. Gao, H. Guo, S. Ha, D. Joseph-McCarthy, L. Kuchnir, K. Kuczera, F. T. K. Lau, C. Mattos, S. Michnick, T. Ngo, D. T. Nguyen, B. Prodhom, W. E. Reiher, III, B. Roux, M. Schlenkrich, J. C. Smith, R. Stote, J. Straub, M. Watanabe, J. Wiórkiewicz-Kuczera, D. Yin, M. Karplus, *J. Phys. Chem. B* **1998**, *102*, 3586–3616.

[53] D. Van Der Spoel, E. Lindahl, B. Hess, G. Groenhof, A. E. Mark, H. J. C. Berendsen, *J. Comput. Chem.* **2005**, *26*, 1701–1718.

[54] W. L. Jorgensen, J. Chandrasekhar, J. Madura, R. W. Impey, M. L. Klein, *J. Chem. Phys.* **1983**, *79*, 926–935.

[55] K. Vanommeslaeghe, E. Hatcher, C. Acharya, S. Kundu, S. Zhong, J. Shim, E. Darian, O. Guvench, P. Lopes, I. Vorobyov, A. D. MacKerell, Jr., *J. Comput. Chem.* **2010**, *31*, 671–690.

[56] T. Darden, D. York, L. G. Pedersen, *J. Chem. Phys.* **1993**, *98*, 10089.

[57] G. Bussi, D. Donadio, M. Parrinello, *J. Chem. Phys.* **2007**, *126*, 014101.

[58] B. R. Brooks, C. L. Brooks III, A. D. MacKerell, Jr., L. Nilsson, R. J. Petrella, B. Roux, Y. Won, G. Archontis, C. Bartels, S. Boresch, A. Caflisch, L. Caves, Q. Cui, A. R. Dinner, M. Feig, S. Fischer, J. Gao, M. Hodoscek, W. Im, K. Kuczera, T. Lazaridis, J. Ma, V. Ovchinnikov, E. Paci, R. W. Pastor, C. B. Post, J. Z. Pu, M. Schaefer, B. Tidor, R. M. Venable, H. L. Woodcock, X. Wu, W. Yang, D. M. York, M. Karplus, *J. Comput. Chem.* **2009**, *30*, 1545–1614.

[59] M. Seeber, M. Cecchini, F. Rao, G. Settanni, A. Caflisch, *Bioinformatics* **2007**, *23*, 2625.

These are not the final page numbers! ↗↗